



Electrosynthesis and characterization of an electrochromic material from poly(1,4-bis(2-thienyl)-benzene) and its application in electrochromic devices

Liany Xu, Jinsheng Zhao*, Chuansheng Cui, Renmin Liu, Jifeng Liu, Huaisheng Wang

Department of Chemistry, Liaocheng University, 252059 Liaocheng, PR China

ARTICLE INFO

Article history:

Received 2 October 2010
Received in revised form
14 December 2010
Accepted 18 December 2010
Available online 28 December 2010

Keywords:

Conjugated polymer
Spectroelectrochemistry
Electrochromic device
Electrochemical polymerization
Poly(1,4-bis(2-thienyl)-benzene)

ABSTRACT

1,4-Bis(2-thienyl)-benzene monomer is successfully synthesized via coupling reaction. Poly(1,4-bis(2-thienyl)-benzene) (PBTB) is electrochemically synthesized and characterized. Resulting polymer film has distinct electrochromic properties. Its application in electrochromic devices (ECDs) is discussed. PBTB is switched between yellow in the neutral state and green in the oxidized state. Electrochromic switching of PBTB film is performed and the polymer film shows a maximum optical contrast ($\Delta T\%$) of 44.8% at 610 nm in visible region with a response time of 1.6 s. The coloration efficiency (CE) of PBTB is calculated to be $162 \text{ cm}^2 \text{ C}^{-1}$. Electrochromic device (ECD) based on PBTB and poly(3,4-ethylenedioxythiophene) (PEDOT) is also constructed and characterized. Maximum contrast ($\Delta T\%$) and switching time of the device are measured as 29.5% and 0.43 s at 628 nm. The CE of the device is calculated to be $408.9 \text{ cm}^2 \text{ C}^{-1}$. Clear change from green (at neutral state) to blue color (at full oxidized state) of this ECD is demonstrated with reasonable cycle life.

© 2010 Elsevier Ltd. All rights reserved.

1. Introduction

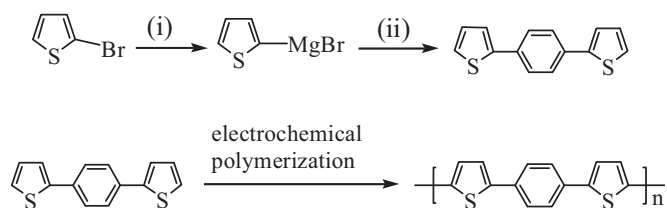
π -Conjugated polymers have attracted much attention because of their promising electronic, optoelectronic and electrochemical properties [1], which can be designed and fabricated by various functional conjugated polymers applied in electronic devices, such as thin-film transistors [2], sensors [3], polymer light-emitting diodes [4], photovoltaics [5], and electrochromic devices [6–8]. Recently, electrochromic (EC) polymers have drawn a lot of attentions due to their outstanding coloration efficiency [9], fast switching times [10], multiple colorations with the same material [11], fine-tunability of the band gap (and the color) [12], high stability [13], thin film flexibility and cost effectiveness [14], which have been widely used in the fields of displays [15], energy-saving “smart” windows [16] and memory devices [17]. For EC polymers, the electrochromism is related to the changing of band gaps during the doping–dedoping process [18,19]. Thus, in order to achieve different properties EC polymers, an effective way is to adjust the electronic character of the π -orbit along the neutral polymer backbone, including main chain and pendant group structural modification and copolymerization [10,19].

In the last years, polymers with a regular alternating arrangement of an aromatic π -electron system are receiving attention for various important technological applications [11]. Amount of

researches about these polymers are focused on their conducting, electroluminescent and photoluminescent properties and their potential application in electronic and electro-optic devices [20,21]. Enhanced delocalization of π -electrons through the π -conjugation on the polymer backbone would improve optical and electric properties of the polymers, including semiconducting properties in the doped state [22].

Among electrochromic materials, thiophenes are a class of important EC conjugated polymers because of their high electrical conductivity and good redox property. They exhibit fast response time, outstanding stability and high contrast ratios in the visible and NIR regions in their electrochromic applications [10]. Moreover, they have facile E_g tunability through structural modification reported extensively in past few years [23,24]. Thus, the electron-rich heterocycles such as thiophene and 3,4-ethylenedioxythiophene (EDOT) are the most common monomers used for electrochemical polymerization. On the other hand, poly(*p*-phenylene) (PPP) is an interesting material for electro-optical applications as its band gap is in the blue region of the visible spectrum and its thermal stability is combined with high photoluminescence [25]. It has been known that the introduction of phenylene bridge in the bithiophene polymer main chains could result in changed HOMO–LUMO band gap polymers compared with both homopolymers [25]. Furthermore, the broad range of substitution possibilities on phenylene rings or on thiophene rings render possibilities to obtain tunable band gap electrochromic materials [25,26]. The electrochromic properties of polymers containing alternating bithiophene and phenylene repeat units have begun to

* Corresponding author. Tel.: +86 635 8324551; fax: +86 635 8239001.
E-mail address: j.s.zhao@163.com (J. Zhao).



Scheme 1. Synthetic routes of monomer and polymer. Reagents: (i) Mg, Et₂O; (ii) 1,4-dibromobenzene, NiCl₂(PPh₃)₂, THF.

draw attentions of researchers [26]. However, to the best of our knowledge, there are still no reports on the fabrication of dual type ECDs based on poly(1,4-bis(2-thienyl)-benzene) (PBTB) and poly(3,4-ethylenedioxythiophene) (PEDOT).

It is well known that the pursuit of new high-quality electrochromic materials is still the main goal of scientists in the field of ECDs. Besides the neutral green polymers, the neutral yellow polymers also showed important values since which can be used to fabricate neutral green dual type ECDs with PEDOT used as the cathodically coloring materials. According to Nie et al., poly(indole-6-carboxylic acid) (PIn) was switched between yellow in the reduced state and green in the oxidized state. Furthermore, the ECD based on PIn and PEDOT was green in its reduced state, short switching time and high optical contrast was also observed [6].

In this study, 1,4-bis(2-thienyl)-benzene (BTB) monomer was synthesized via coupling reaction according to the report in the literature [27]. In this BTB monomer structure, the para position substitutions (thiophene) of the phenylene ring modify the degree of conjugation (extended π - π^* bonding system) [28]. Due to the conjugated structures of the corresponding monomers, poly(1,4-bis(2-thienyl)-benzene) can be easily achieved by electrochemical polymerization of 1,4-bis(2-thienyl)-benzene monomer in common organic solution with a much lower oxidation potentials than that of thiophene [29]. The resultant polymer film presents unique electrochromic property (yellow color at neutral state and green color at full doped state) due to the introduction of phenylene units into poly(2,2-bithiophene) backbone. The obtained PBTB polymer is characterized via cyclic voltammetry, SEM, UV-vis and FT-IR spectra. The spectroelectrochemical and electrochromic properties of the PBTB and its dual type polymer ECDs constructed with PEDOT are also investigated in details. The results of the study show that PBTB is also a good candidate for fabrication of neutral green ECDs.

2. Experimental

2.1. Materials

1,4-Dibromobenzene, 2-bromothiophene and 3,4-ethylenedioxythiophene (EDOT, 98%) are all purchased from Aldrich Chemical and used as received. Commercial high-performance liquid chromatography grade acetonitrile (ACN, Tedia Company, Inc., USA) are used directly without further purification. Sodium perchlorate (NaClO₄, Shanghai Chemical Reagent Company, 98%) is dried in vacuum at 60 °C for 24 h before use. Other reagents are all used as received without further treatment.

2.2. Synthesis of 1,4-bis(2-thienyl)-benzene

The 1,4-bis(2-thienyl)-benzene (BTB) monomer was synthesized according to the procedure reported before by Yang et al. [27]. As shown in Scheme 1, 2-bromothiophene is reacted with magnesium to afford Grignard reagents which are then cross-coupled to 1,4-dibromobenzene in the presence of cat-

alytic bis(triphenylphosphino) dichloronickel(II) (NiCl₂(PPh₃)₂). The purified product is an orange-yellow crystal. ¹H NMR and FT-IR spectra verified the structure and purity of the BTB monomer.

2.3. Instrumentation

¹H NMR spectroscopy studies are carried out on a Varian AMX 400 spectrometer and tetramethylsilane (TMS) is used as the internal standard for ¹H NMR. FT-IR spectra are recorded on a Nicolet 5700 FT-IR spectrometer, where the samples are dispersed in KBr pellets. UV-vis spectra are measured with a Perkin-Elmer Lambda 900 UV-vis-near-infrared spectrophotometer. Scanning electron microscopy (SEM) measurements are taken by using a JEOL JSM-6380LV SEM. The photographs of electrochromic films and device cell are taken by a Fujifilm Shot (FinePix F200EXR) digital camera.

2.4. Electrochemistry

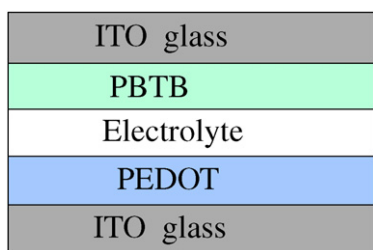
Electrochemical synthesis and experiments is carried out in a one-compartment cell with a CHI 760 C Electrochemical Analyzer under computer control, employing a platinum wires with a diameter of 0.5 mm as working electrode, a platinum ring as counter electrode, and a silver wire (Ag wire) as pseudo reference electrode. The working and counter electrodes for cyclic voltammetric experiments are placed 0.5 cm apart during the experiments. The electrolytes used are 0.2 M of NaClO₄ in ACN solution. The electrodeposition is performed from a 0.004 M solution of the monomer in the electrolyte potentiodynamically at a scan rate of 100 mV s⁻¹ or potentiostatically at +1.30 V vs. Ag wire. The pseudo reference is calibrated externally using a 5 mM solution of ferrocene (Fc/Fc⁺) in the electrolyte ($E_{1/2}(\text{Fc}/\text{Fc}^+) = +0.20$ V vs. Ag wire in 0.2 M NaClO₄/ACN) [10]. The half-wave potential ($E_{1/2}$) of Fc/Fc⁺ measured in 0.2 M NaClO₄/ACN solution is 0.28 V vs. SCE. Thus, the potential of Ag wire was assumed to be +0.08 V vs. SCE. Cyclic voltammetry of polymer is carried out using the same electrode set-up in monomer-free electrolyte solution. All of the electrochemistry experiments are carried out at room temperature under nitrogen atmosphere.

2.5. Spectroelectrochemistry

Spectroelectrochemical data are recorded on Perkin-Elmer Lambda 900 UV-vis-near-infrared spectrophotometer connected to a computer. A three-electrode cell assembly is used where the working electrode is an ITO-coated glass slides (sheet resistance: < 10 Ω \square^{-1} , purchased from Shenzhen CSG Display Technologies (China)), the counter electrode is a stainless steel wire, and an Ag wire is used as pseudo reference electrode. The potentials are reported vs. Ag wire. Polymer films for spectroelectrochemistry are prepared by potentiostatically deposition on ITO-coated (the active area: 2.1 cm \times 0.8 cm) glass slides.

2.6. Preparation of the gel electrolyte

A gel electrolyte based on poly(methyl methacrylate) (PMMA) (MW: 350,000) and LiClO₄ is plasticized with propylene carbonate (PC) to form a highly transparent and conductive gel. ACN is also included as a high vapor pressure solvent to allow an easy mixing of the gel components. The composition of the casting solution by weight ratio of ACN:PC:PMMA:LiClO₄ is 70:20:7:3. The gel electrolyte is used for construction of the polymer electrochromic device cell [9].



Scheme 2. Multi-layers structure of ECD.

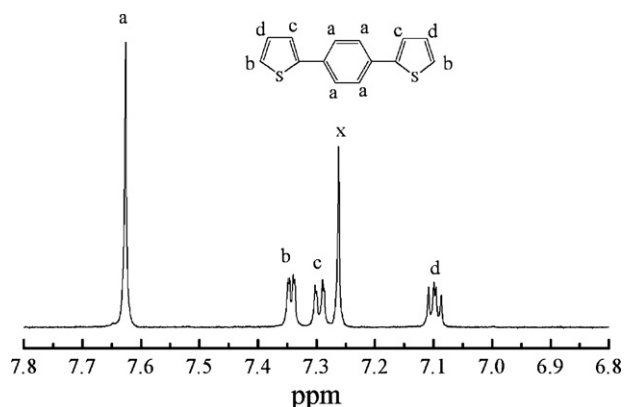


Fig. 1. ^1H NMR spectrum of 1,4-bis(2-thienyl)-benzene monomer in CDCl_3 . Solvent peak at $\delta = 7.262$ ppm is marked 'x'.

2.7. Construction of ECDs

ECDs are constructed using two complementary polymers, namely PBTB as the anodically coloring material and PEDOT as the cathodically coloring material (Scheme 2). The PBTB and PEDOT films were electrochemically deposited on ITO electrodes ($1.8\text{ cm} \times 2.4\text{ cm}$) at 1.3 and 1.4 V with the charges of $2.5 \times 10^{-2}\text{ C}$ and $3.5 \times 10^{-2}\text{ C}$, respectively. ECDs are built by arranging the two polymer films (one oxidized, the other reduced) facing each other separated by a gel electrolyte (Scheme 2). The spectroelectrochemical measurements of the ECD are undertaken after the evaporation of ACN in 24 h.

3. Results and discussion

3.1. ^1H NMR spectrum, FTIR spectra of BTB monomer

^1H NMR spectrum of BTB (Fig. 1): $\text{C}_{14}\text{H}_{10}\text{S}_2$, δ_{H} (CDCl_3) 7.626 (s, 4H), 7.343 (d, 2H), 7.294 (d, 2H), 7.097 (t, 2H). The protons of phenylene ring are observed at 7.626 ppm. The protons of thiophene ring are at 7.343 (α -proton), 7.294 (β -proton) and 7.097 ppm (β -proton), respectively.

FT-IR spectrum of BTB is shown in Fig. 4a. In the spectrum of BTB, the bands around 1599 and 1542 cm^{-1} are ascribed to the stretching vibrations of phenylene rings, and the bands at 1497 and 1458 cm^{-1} are due to the stretching vibrations of thiophene rings [19,30]. Two strong peaks located at 699 cm^{-1} and 815 cm^{-1} are assigned to the out-of-plane bending vibrations of C–H bonding in the monosubstituted thiophene rings and in the 1,4-disubstituted phenylene rings, respectively [31].

3.2. Electrochemical polymerization and characterization of PBTB

3.2.1. Electrochemical polymerization of PBTB

The successive CV curves of 0.004 M BTB in 0.2 M $\text{NaClO}_4/\text{ACN}$ are illustrated in Fig. 2. The onset oxidation potential ($E_{\text{pa onset}}$) of

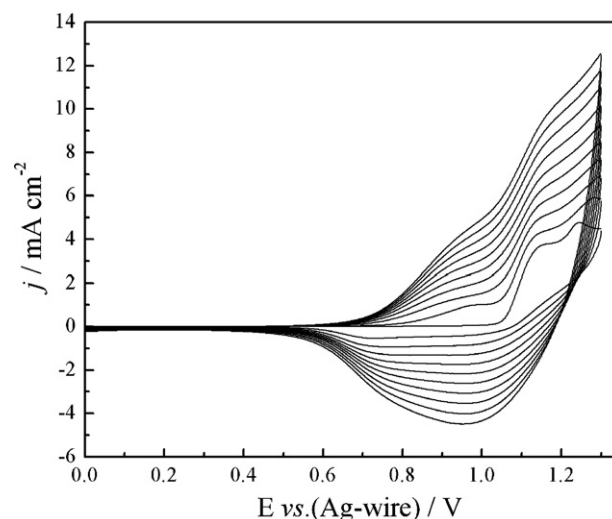


Fig. 2. Cyclic voltammogram curves of 0.004 M BTB in 0.2 M $\text{NaClO}_4/\text{ACN}$ solutions at a scan rate of 100 mV s^{-1} .

BTB in the solution is 1.05 V (Fig. 2), which is lower than that of 2,2'-bithiophene monomer (1.11 V) in the same electrolyte solution [32]. As the CV scan continued, polymer films are formed on the working electrode surface. The increases in the redox wave current densities imply that the amount of conducting polymers deposited on the electrode are increasing [33]. The CV curves of BTB show distinct reduction waves of the oligomer located at 0.95 V, while the corresponding oxidation waves are overlapped with the oxidation waves of the BTB monomer and cannot be observed clearly [34].

3.2.2. Electrochemistry behavior of the polymer films

Fig. 3 shows the electrochemical behavior of the PBTB film (prepared on platinum wires by sweeping the potentials from 0 to +1.3 V for three cycles) at different scan rates between 50 and 300 mV s^{-1} in 0.2 M $\text{NaClO}_4/\text{ACN}$. As can be seen from Fig. 3a, the PBTB film is cycled repeatedly between doped and dedoped states without significant decomposition. The peak current densities (j) are proportional to the potential scan rates (Fig. 3b), indicating a reversible redox process of the polymer adheres well to the platinum wire electrode [34]. This also demonstrates that the electrochemical processes of the polymer are reversible and not diffusion limited [35,36].

3.2.3. FTIR spectrum of PBTB

To obtain a sufficient amount of PBTB for characterization, the ITO glass with a surface area of 1.6 cm^2 is employed as working electrodes. The polymer is synthesized at +1.3 V vs. Ag wire potentiostatically in the solution of 0.2 M $\text{NaClO}_4/\text{ACN}$ containing 0.004 M monomer. Fig. 4b shows the FT-IR spectrum of PBTB. The absorption peaks at 792 and 1050 cm^{-1} are attributed to the out-of-plane and in-plane bending vibrations of C–H bonding in β -position of the 2,5-disubstituted thiophene rings, respectively [37]. Compared with the spectrum of BTB, the disappearance of the out-of-plane C–H bending vibrations of mono-substituted thiophene rings at 699 cm^{-1} implies that the polymerization occurs at the α -position of thiophene rings (see Scheme 1).

3.2.4. Scanning electron microscopy of PBTB film

The polymer film of PBTB is prepared potentiostatically at +1.3 V vs. Ag wire from the solution of 0.2 M $\text{NaClO}_4/\text{ACN}$ containing 0.004 M monomer on ITO electrode. The surface morphology of the neutral PBTB is investigated by scanning electron microscopy (SEM) after dedoping at -0.1 V for 10 min in 0.2 M $\text{NaClO}_4/\text{ACN}$. The

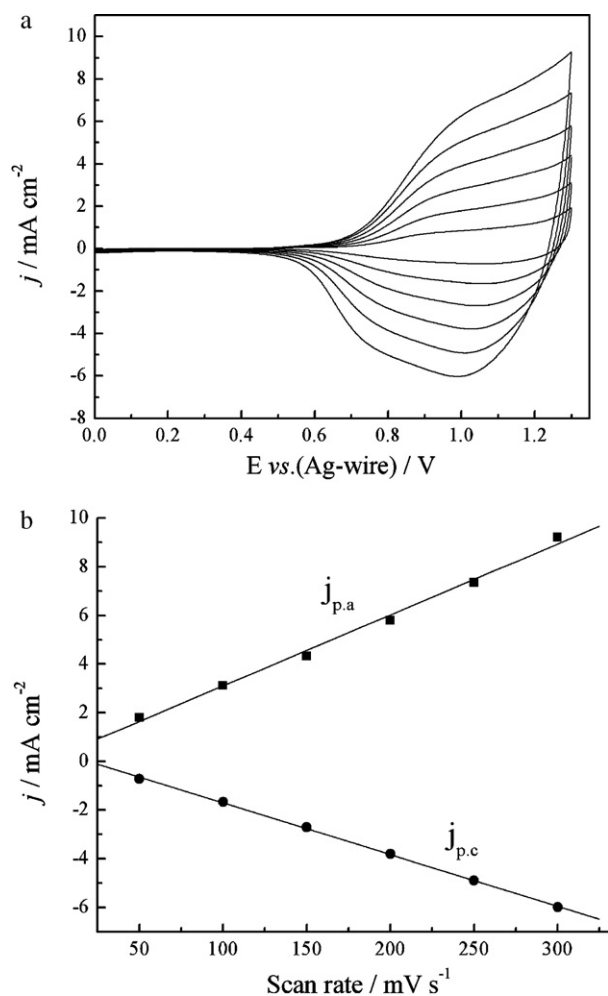


Fig. 3. (a) CV curves of the PBTB film at different scan rates between 30 mV s^{-1} and 300 mV s^{-1} in the monomer-free $0.2 \text{ M NaClO}_4/\text{ACN}$. (b) Scan rate dependence of the PBTB. $j_{p,a}$ and $j_{p,c}$ denote the anodic and cathodic peak current densities, respectively.

PBTB film exhibits compact structure and globules like droplets are dispersed on the side of PBTB film (Fig. 5), and the approximate diameters of these globules are in the range of 500–1000 nm.

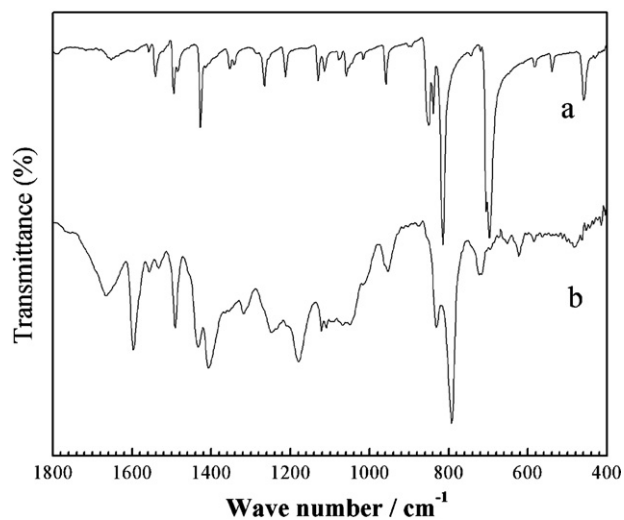


Fig. 4. The FT-IR spectra of (a) 1,4-bis(2-thienyl)-benzene monomer and (b) PBTB prepared at +1.30 V potentiostatically.

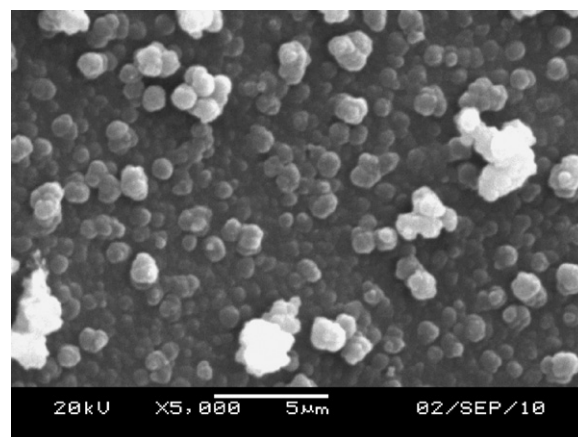


Fig. 5. SEM images of PBTB deposited on ITO electrode at +1.3 V potentiostatically.

3.2.5. Optical properties of BTB monomer and PBTB film

The UV–vis spectra of BTB and 2,2'-bithiophene (BT) monomers in CH_2Cl_2 solution are shown in Fig. 6a, and the UV–vis spectra of PBTB and poly(2,2'-bithiophene) (PBT) deposited on ITO electrodes are also shown in Fig. 6b. As can be seen from Fig. 6a, BTB shows a strong and sharp absorption peak at 324 nm (Fig. 6a), which exhibits a 22 nm red shift compared with that of BT at 302 nm due to the extended degree of conjugation (π – π^* bonding system) by the

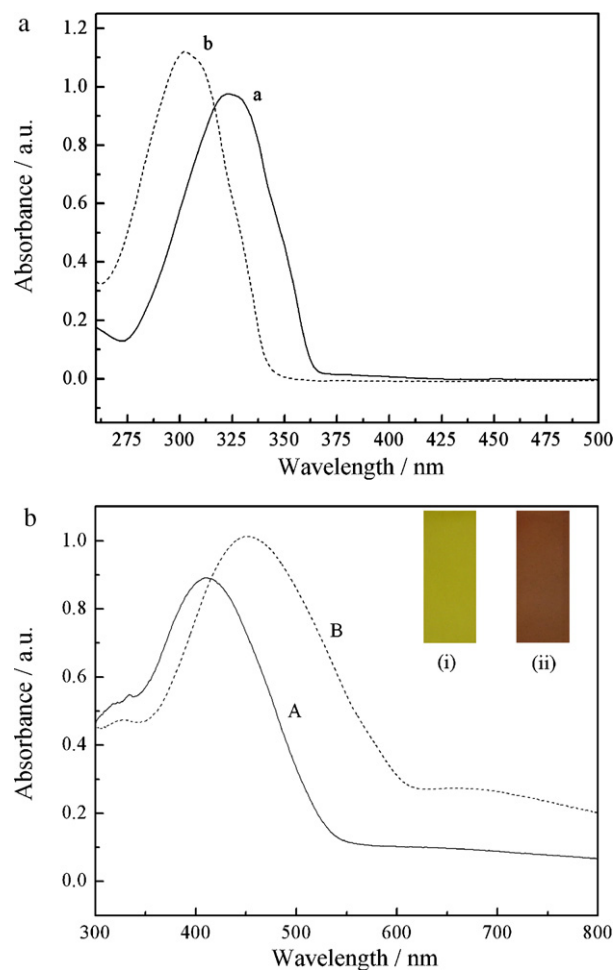


Fig. 6. UV–vis spectra of (a) BTB and BT dissolved in CH_2Cl_2 and (b) PBTB and PBT deposited on ITO electrode. Insert: the images of (i) PBTB and (ii) PBT film at the neutral state.

Table 1The onset oxidation potential (E_{onset}), HOMO and LUMO energy levels and optical band gap (E_g) of BTB, BT, PBTB and PBT.

Compounds	E_{onset} , vs. (Ag-wire) (V)	λ_{max} (nm)/ λ_{edge} (nm)	E_g (eV)	HOMO (eV)	LUMO ^a (eV)
BTB	1.05	324/364	3.41	-5.53	-2.12
BT	1.11	302/342	3.63	-5.59	-1.96
PBTB	0.72	411/535	2.31	-5.20	-2.89
PBT	0.91	450/607	2.04	-5.39	-3.35

^a Calculated by the subtraction of the optical band gap from the HOMO level.

introduction of phenylene bridge into the BT monomer. In Fig. 6b, UV-vis spectrum of PBTB exhibits an absorption band with a maximum at 411 nm attributed to π - π^* transition of PBTB. There is a 39 nm blue shift compared to that of PBT at 450 nm, which might be caused by the lower degree of conjugation of PBTB than that of PBT due to the incorporation of the rigid phenylene moieties into polymer main chains. The increase in the main-chain rigidity of PBTB than that of PBT would decrease the degree of polymerization and then the length of the conjugated chain (i.e., conjugation degree), which is proved by lower onset temperature of weight loss of PBTB than that of PBT (350 °C vs. 541 °C, the thermogravimetry curves was not shown). In the dedoped state, PBTB film on ITO is yellow color (the insert (i) of Fig. 6b) and PBT film is brown red color (the insert (ii) of Fig. 6b). The difference between the colors of PBTB and PBT film can be attributed to the blue shift of the π - π^* transition absorption band of PBTB compared to that of PBT.

Table 1 summarizes the electronic absorption, the onset oxidation potential (E_{onset}) and the optical band gap (E_g) of the BTB, BT, PBTB and PBT quite clearly. HOMO energy levels of them are calculated by using the formula $E_{\text{HOMO}} = -e(E_{\text{onset}} + 4.4)$ (E_{onset} vs. SCE) and LUMO energy levels (E_{LUMO}) of them are calculated by the subtraction of the optical band gap from the HOMO levels [38,39]. The low energy edge of the absorption spectrum (λ_{edge}) of BTB is at 364 nm which corresponds to optical band gap (E_g) of 3.41 eV. For PBTB, it is observed at 535 nm corresponding to a band gap of 2.31 eV. The values of the band gap for PBTB lies between 3.0 eV for poly(*p*-phenylene) (PPP) and 2.04 eV for PBT [40], indicating that the alternating introduction of 2,2'-thiophene units into copolymer main chain could lead to an obvious decrease in the E_g for PBTB compared with that of PPP.

3.3. Electrochromic properties of PBTB

3.3.1. Spectroelectrochemical properties of PBTB

Spectroelectrochemistry is used to obtain information about the electronic structure of PBTB and to examine the spectral changes which occur during redox switching. PBTB coated ITO (prepared potentiostatically at +1.30 V vs. Ag wire) is switched between 0 and +1.30 V in 0.2 M NaClO₄/ACN system in order to obtain the in situ UV-vis spectra (Fig. 7). In the neutral state, polymer film exhibits an absorption peak at 411 nm due to the π - π^* transition. Upon oxidation, the intensity of the π - π^* transition reduce and the simultaneous increase of absorbance at 610 nm can be observed.

The colors of the electrochromic materials are defined accurately by performing colorimetry measurements. CIE system is used as a quantitative scale to define and compare colors. Three attributes of color: hue (*a*), saturation (*b*) and luminance (*L*) are measured and recorded. The PBTB film on ITO electrode has distinct electrochromic properties. During the oxidation process, yellow color of the film at neutral state turns into green color at full doped state. These colors and corresponding *L*, *a*, *b* values are given in Fig. 7 (see insets).

3.3.2. Electrochromic switching of PBTB film in solution

It is important that polymers can switch rapidly and exhibit striking color changes, revealing superior results in electrochromic

applications [6]. The dynamic electrochromic experiment for PBTB is carried out at 610 nm, where the maximum transmittance differences between redox states are observed in the visible region. Double potential step chronoamperometry technique is coupled with optical spectroscopy, to investigate the switching ability of PBTB between its neutral and doped state (Fig. 8) [41]. The potential is interchanged between 0 (the neutral state) and +1.3 V (the oxidized state) at regular intervals of 4 s. One important characteristic is the optical contrast (ΔT %), which can be defined as the transmittance difference between the redox states. The ΔT % of the PBTB is found to be 44.8% at 610 nm, as showed in Fig. 8b.

The coloration efficiency (CE) is also an important characteristic for the electrochromic materials. CE can be calculated by using the equations and given below [42]:

$$\Delta OD = \lg \left(\frac{T_b}{T_c} \right) \quad \text{and} \quad \eta = \frac{\Delta OD}{\Delta Q}$$

where T_b and T_c are the transmittances before and after coloration, respectively. ΔOD is the change of the optical density, which is proportional to the amount of created color centers. η denotes the coloration efficiency (CE). ΔQ is the amount of injected charge per unit sample area. CE of PBTB film is measured as 162 cm² C⁻¹ (at 610 nm) at full doped state, which had reasonable coloration efficiency.

Response time, one of the most important characteristics of electrochromic materials, is the time needed to perform a switching between the neutral state and oxidized state of the materials [6,36]. The response required to attain 95% of total transmittance difference is found to be 1.6 s from the reduced to the oxidized state and 0.54 s from the oxidized to the reduced state. Thus, PBTB can be rapidly switched to the reduced state, which can be attributed to the ease of charge transport in the conducting film when it is

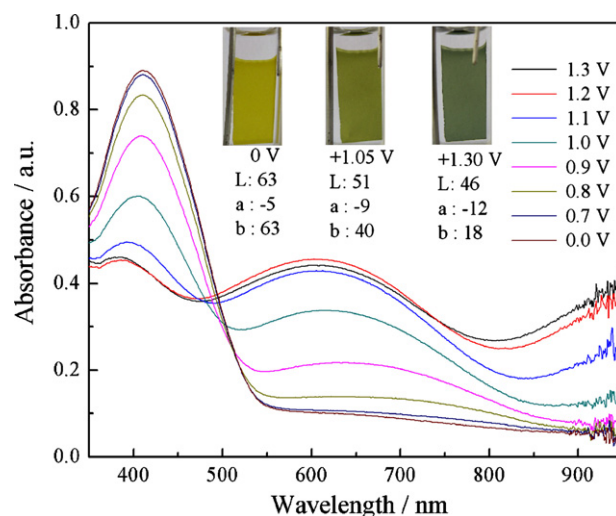


Fig. 7. Spectroelectrochemical spectra of PBTB with applied potentials between 0 V and +1.3 V in 0.2 M NaClO₄/ACN. Insert: the images of poly film at 0 V (the neutral state), +1.05 V (the intermediate state) and +1.30 V (the full doped state).

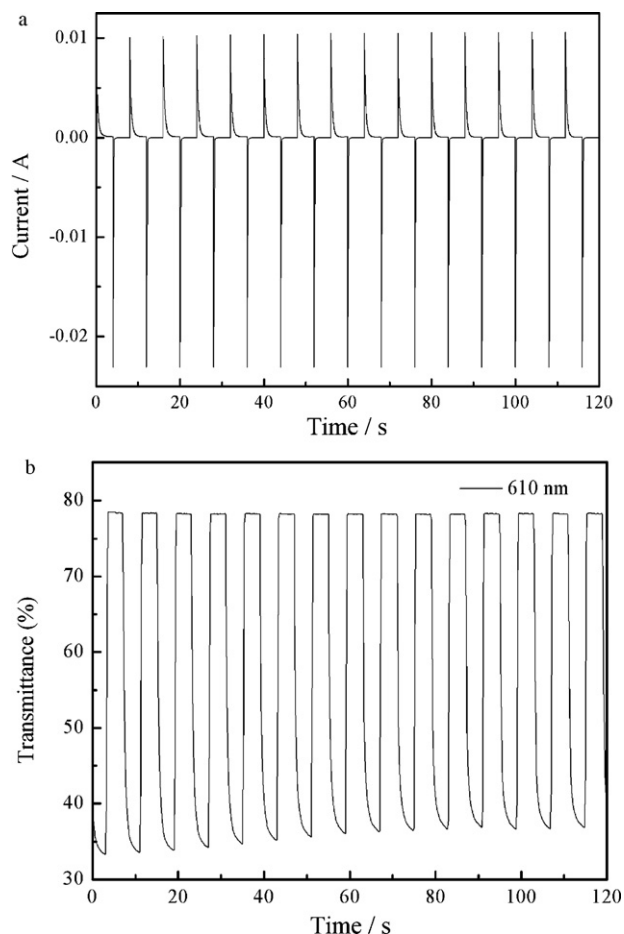


Fig. 8. Electrochromic switching (610 nm) and electrical current response for PBTB film monitored in 0.2 M $\text{NaClO}_4/\text{ACN}$ solution under an applied potentials between 0V and 1.3 V at regular intervals of 4s. (a) Current response and (b) optical response.

reduced [43]. Based on the discussion, these properties make PBTB a promising electrochromic material [10].

3.4. Spectroelectrochemistry of electrochromic devices (ECDs)

3.4.1. Spectroelectrochemical properties of ECD

A dual type ECD consisting of PBTB and PEDOT is constructed and its spectroelectrochemical behaviors are also studied. Before composing the ECD, the cathodically coloring polymer (PEDOT) is fully oxidized while the anodically coloring polymer film (PBTB) is fully reduced. PBTB/PEDOT ECD is switched between -0.8 and $+1.5$ V. The spectroelectrochemical results show PBTB layer is in its neutral state and PEDOT is in oxidized state at -0.8 V, and the device color is green (Fig. 9). As the applied potential increased, the PBTB layer start to be oxidized while PEDOT layer is reduced, which lead to a new absorption at 628 nm due to the reduced state of PEDOT, and the dominated color of the device is blue at $+1.5$ V (Fig. 9).

3.4.2. Switching of ECD

Kinetic studies are also done to test the response time of PBTB/PEDOT ECD. While switching the potential between -0.8 and $+1.5$ V with a residence time of 2 s, the optical response at 628 nm and the electrical current response of the device are recorded at the same time, as illustrated in Fig. 10 (the figure of the electrical current response is not shown). The response time is found to be 0.43 s at 95% of the maximum transmittance difference from the neutral state to oxidized state and 0.21 s from the oxidized state

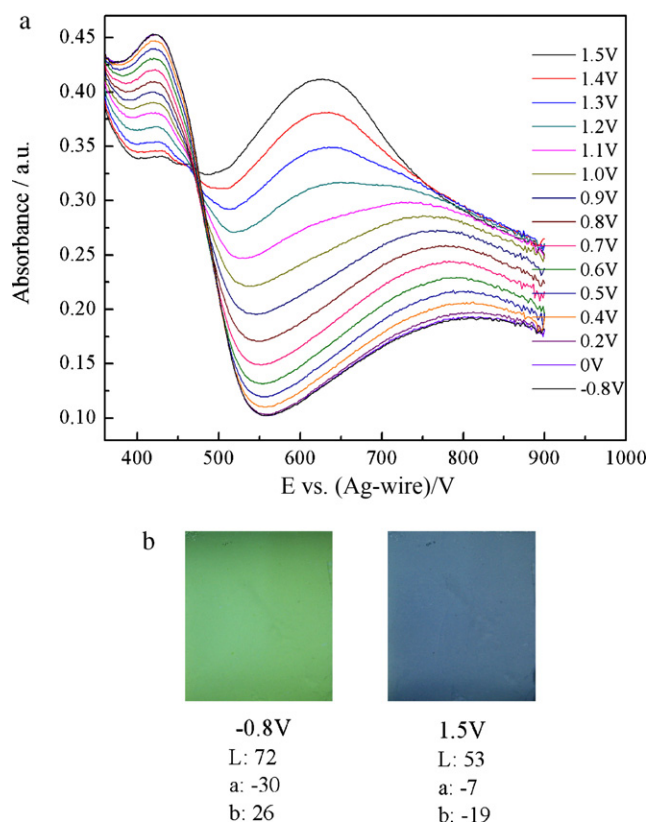


Fig. 9. (a) Spectroelectrochemical spectra of PBTB/PEDOT device at various applied potentials from -0.8 to $+1.5$ V and (b) the colors of the device at -0.8 V (the neutral state) and $+1.3$ V (the oxidized state).

to the neutral state, and $\Delta T\%$ is calculated to be 29.5%. The CE of the device (the active of area is $1.8 \text{ cm} \times 1.8 \text{ cm}$) is calculated to be $408.9 \text{ cm}^2 \text{ C}^{-1}$, a high and advantageous value, especially for large area devices.

3.4.3. Open circuit memory of ECD

The optical memory in the electrochromic devices is an important parameter since it is directly related to its application and energy consumption during the use of ECDs [44]. The optical spec-

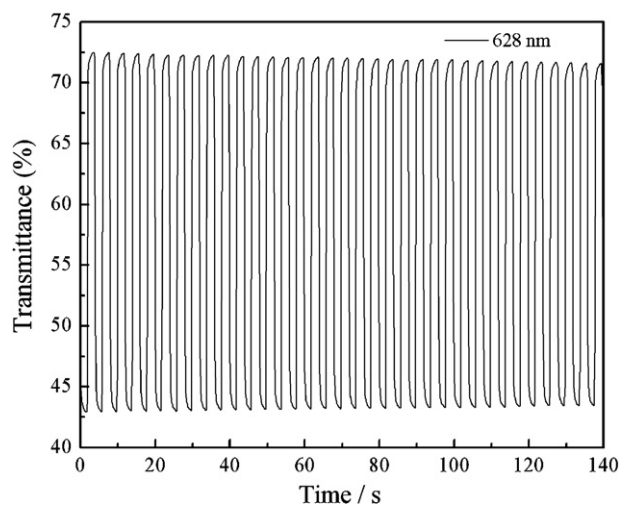


Fig. 10. Optical response (at 628 nm) as a function of time of PBTB/PEDOT device by applying potentials between -0.8 V (the neutral state) and $+1.5$ V (the oxidized state) at regular intervals of 2 s.

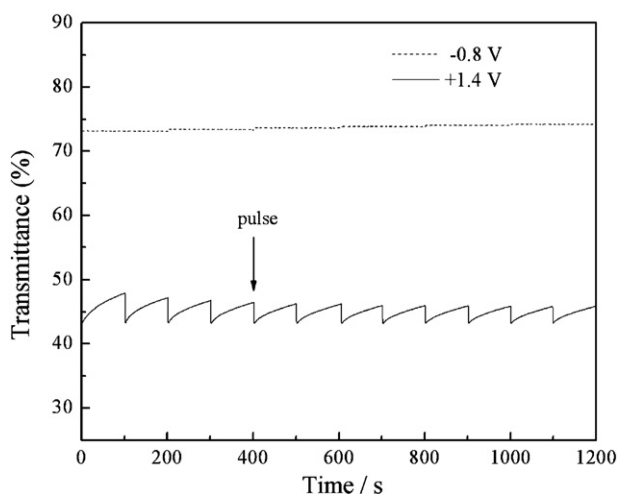


Fig. 11. Open circuit stability of the PBTB/PEDOT ECD monitored at 628 nm.

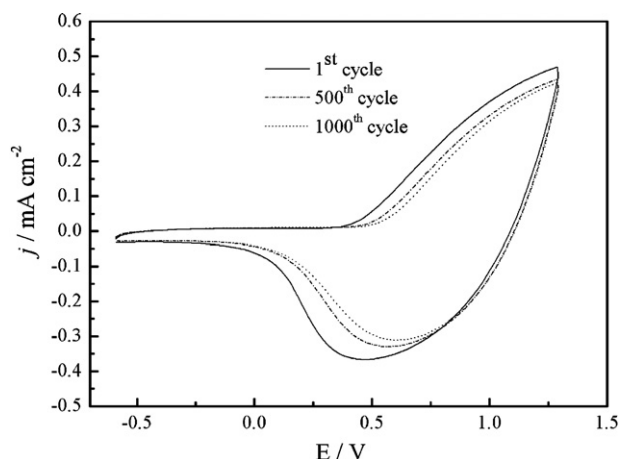


Fig. 12. Cyclic voltammogram of PBTB/PEDOT device as a function of repeated scans 500 mV s⁻¹.

tra for PBTB is monitored at 628 nm as a function of time at -0.8 and $+1.4$ V by applying the potential for 1 s for 200 and 100 s time intervals, respectively. As seen in Fig. 11, both blue and green states are highly stable and the device keeps its color without significant loss. Thus, this device shows a good optical memory. Based on this discussion, PBTB/PEDOT ECD is well performing under open circuit conditions, indicating this ECD has potential applications.

3.4.4. Stability of ECD

Redox stability is another important parameter for ECDs. The stability of devices toward multiple redox switching usually limits the application of electrochromic materials in ECD utility [6]. For this reason, the PBTB/PEDOT ECD is tested by cycling of the applied potential between -0.6 and $+1.3$ V with 500 mV s⁻¹ to evaluate the stability of the devices (Fig. 12). After 500 cycles, 86.0% of its electroactivity is retained and there is no obvious decrease of activity between 500 cycles and 1000 cycles. These results indicate that this ECD has reasonable redox stability.

4. Conclusions

1,4-Dis(2-thienyl)-benzene monomer containing benzene and thiophene units is synthesized by coupling reaction and then its polymer is successfully synthesized by electrochemical oxida-

tion of the monomer in 0.2 M NaClO₄/ACN solution. The obtained polymer film is studied by cyclic voltammetry, UV-vis and FT-IR spectra, scanning electron microscopy. Electrochromic properties of PBTB film are investigated in detail. Spectroelectrochemistry reveals that PBTB film has good electrochromic properties (yellow color at neutral state and green color at full doped state). The dual type ECD constructed utilizing PBTB and PEDOT has reasonable response time (0.43 s) and optical contrast (29.5%) at 628 nm. The CE of the ECD is calculated to be 408.9 cm² C⁻¹. It is interesting that this ECD shows green color at neutral state. These properties make PBTB a good candidate for commercial applications.

Acknowledgements

Financial supports from the National Natural Science Foundation of China (no. 20906043) and the Taishan Scholarship of Shandong Province are gratefully acknowledged.

References

- [1] S. Gunes, H. Neugebauer, N.S. Sariciftci, *Chem. Rev.* 107 (2007) 1324.
- [2] J.J.M. Halls, C.A. Walsh, N.C. Greenham, E.A. Marseglia, R.H. Friend, S.C. Moratti, A.B. Holmes, *Nature* 376 (1995) 498.
- [3] D.T. McQuade, A.E. Pullen, T.M. Swager, *Chem. Rev.* 100 (2000) 2537.
- [4] R.H. Friend, R.W. Gymer, A.B. Holmes, J.H. Burroughes, R.N. Marks, C. Taliani, D.D.C. Bradley, D.A. Dos Santos, J.L. Bredas, M. Logdlund, W.R. Salaneck, *Nature* 397 (1999) 121.
- [5] C.J. Brabec, N.S. Sariciftci, J.C. Hummelen, *Adv. Funct. Mater.* 11 (2001) 15.
- [6] G.M. Nie, L.J. Zhou, Q.F. Guo, S.S. Zhang, *Electrochem. Commun.* 12 (2010) 160.
- [7] O. Turkarslan, M. Ak, C. Tanyeli, I.M. Akhmedov, L. Toppare, *J. Polym. Sci. Part A: Polym. Chem.* 45 (2007) 4496.
- [8] S. Koyuncu, B. Gultekin, C. Zafer, H. Bilgili, M. Can, S. Demic, İ. Kaya, S. Icli, *Electrochim. Acta* 54 (2009) 5694.
- [9] G. Sonmez, H. Meng, F. Wudl, *Chem. Mater.* 16 (2004) 574.
- [10] G. Sonmez, C.K.F. Shen, Y. Rubin, F. Wudl, *Angew. Chem. Int. Ed.* 43 (2004) 1498.
- [11] A. Yildirim, S. Tarkuc, M. Ak, L. Toppare, *Electrochim. Acta* 53 (2008) 4875.
- [12] E. Yildiz, P. Camurlu, C. Tanyeli, I. Akhmedov, L. Toppare, *J. Electroanal. Chem.* 612 (2008) 247.
- [13] M. Li, A. Patra, Y. Sheynin, M. Bendikov, *Adv. Mater.* 21 (2009) 1707.
- [14] C. Ma, M. Taya, C.Y. Xu, *Electrochim. Acta* 54 (2008) 598.
- [15] R.J. Mortimer, A.L. Dyer, J.R. Reynolds, *Displays* 27 (2006) 2.
- [16] A. Azens, C.G. Granqvist, *J. Solid State Electrochem.* 7 (2003) 64.
- [17] S. Möller, C. Perlov, W. Jackson, C. Taussig, S.R. Forrest, *Nature* 426 (2003) 166.
- [18] F.B. Koyuncu, S. Koyuncu, E. Ozdemir, *Electrochim. Acta* 55 (2010) 4935.
- [19] C. Zhang, C. Hua, G.H. Wang, M. Ouyang, C.A. Ma, *J. Electroanal. Chem.* 645 (2010) 50.
- [20] J. Seixas de Melo, J. Pina, H.D. Burrows, R.E. Di Paolo, A.L. Maçanita, *Chem. Phys.* 330 (2006) 449.
- [21] A. Bessiere, C. Duhamel, J.C. Badot, V. Lucas, M.C. Certiat, *Electrochim. Acta* 49 (2004) 2051.
- [22] S.A. Manhart, A. Adachi, K. Sakamaki, K. Okita, J. Ohshita, T. Ohno, T. Hamaguchi, A. Kunai, J. Kido, *J. Organomet. Chem.* 592 (1999) 52.
- [23] C. Pozzo-Gonzalo, M. Salsamendi, J.A. Pomposo, H.J. Grande, E.Y. Schmidt, Y.Y. Rusakov, B.A. Trofimov, *Macromolecules* 41 (2008) 6886.
- [24] Y. Pang, X. Li, H. Ding, G. Shi, L. Jin, *Electrochim. Acta* 52 (2007) 6172.
- [25] L. Akcelrud, *Prog. Polym. Sci.* 28 (2003) 875.
- [26] S.C. Ng, J.M. Xu, H.S.O. Chan, *Synth. Met.* 110 (2000) 31.
- [27] M.J. Yang, Q.H. Zhang, P. Wu, H. Ye, X. Liu, *Polymer* 46 (2005) 6266.
- [28] S. Ayachi, K. Alimi, M. Bouachrine, M. Hamidi, J.Y. Mevellec, J.P. L'ere-Porte, *Synth. Met.* 156 (2006) 318.
- [29] A. Durmus, G.E. Gunbas, P. Camurlu, L. Toppare, *Chem. Commun.* 31 (2007) 3246.
- [30] S.C. Ng, J.M. Xu, H.S.O. Chan, A. Fujii, K. Yoshino, *J. Mater. Chem.* 9 (1999) 381.
- [31] S. Jin, S. Cong, G. Xue, B. Mansdorf, S.Z.D. Cheng, *Adv. Mater.* 14 (2002) 1492.
- [32] L.Y. Xu, J.S. Zhao, R.M. Liu, H.T. Liu, J.F. Liu, H.S. Wang, *Electrochim. Acta* 55 (2010) 8855.
- [33] R. Yue, J.K. Xu, B.Y. Lu, C.C. Liu, Y.Z. Li, Z.J. Zhu, S. Chen, *J. Mater. Sci.* 44 (2009) 5909.
- [34] G.W. Lu, G.Q. Shi, *J. Electroanal. Chem.* 586 (2006) 154.
- [35] C. Zhang, Y. Xu, N. Wang, Y. Xu, W. Xiang, M. Ouyang, C. Ma, *Electrochim. Acta* 55 (2009) 13.
- [36] B. Yigitsoy, S. Varis, C. Tanyeli, I.M. Akhmedov, L. Toppare, *Electrochim. Acta* 52 (2007) 6561.
- [37] K. Kham, S. Sadki, C. Chevrot, *Synth. Met.* 145 (2004) 135.
- [38] D.M. de Leeuw, M.M.J. Simenon, A.R. Brown, R.E.F. Einerhand, *Synth. Met.* 87 (1997) 53.

- [39] Y.F. Li, Y. Cao, J. Gao, D.L. Wang, G. Yu, A.J. Heeger, *Synth. Met.* 99 (1999) 243.
- [40] J.R. Reynolds, J.P. Ruiz, A.D. Child, K. Nayak, D.S. Marynick, *Macromolecules* 24 (1991) 678.
- [41] E. Sefer, F.B. Koyuncu, E. Oguzhan, S. Koyuncu, *J. Polym. Sci. Part A: Polym. Chem.* 48 (2010) 4419.
- [42] C. Bechinger, M.S. Burdis, J.-G. Zhang, *Solid State Commun.* 101 (1997) 753.
- [43] G.A. Sotzing, J.R. Reynolds, *Chem. Mater.* 8 (1996) 882.
- [44] W.A. Gazotti, J.R.G. Casalbore-Micelli, A. Geri, M.A. De-Paoli, *Adv. Mater.* 10 (1998) 60.